


ORIGINAL ARTICLE

SEM technology for the analysis of tiny calcified remains from a pre-Hispanic burial from El Hierro (Canary Islands)

Alejandra C. Ordóñez^{1,2}  | Emma Suárez-Toste³ |
 Samuel Cockerill¹ | Emilio González-Reimers⁴ |
 Matilde Arnay-de-la-Rosa¹

¹G.I. Tarha, Departamento de Ciencias Históricas, Universidad de Las Palmas de Gran Canaria (ULPGC), Las Palmas, Spain

²Departamento de Geografía e Historia, Universidad de La Laguna (ULL), Tenerife, Canary Islands, Spain

³General Service Research Support (SEGAI), Universidad de La Laguna, Tenerife, Canary Islands, Spain

⁴Grupo de Investigación ULL “Bioantropología, Paleopatología, Dieta y Nutrición en poblaciones antiguas”, Universidad de La Laguna, Tenerife, Islas Canarias, Spain

Correspondence

Alejandra C. Ordóñez, Departamento de Geografía e Historia, Universidad de La Laguna (ULL), Tenerife, Canary Islands, Spain.

Email: alejandra.calderon@ulpgc.es

Funding information

Universidad de Las Palmas de Gran Canaria (ULPGC)

Abstract

Scanning electron microscopy (SEM) coupled with energy-dispersive X-ray spectroscopy (EDX) enables the determination of the composition and structure of tiny calcified remains occasionally recovered during burial excavations. To deepen the practical application of this technique, we performed SEM/EDX analysis on three different tiny mineralized, roughly rounded structures with a diameter of less than 5 mm recovered from a pre-Hispanic collective funerary cave from El Hierro (Canary Islands) and a mineral spherulite of similar size and outer aspect. After SEM imaging and spectroscopic analysis, we conclude that the three samples represent a sesamoid bone, a kidney stone, and a possible case of sialolithiasis. In contrast, the spherulite is a mineral formation composed of calcium carbonate. Our data confirm SEM analysis's usefulness in identifying small, mineralized remains recovered during burial excavations and its contribution to studying past populations. However, we are aware that taphonomic changes may alter, at least partially, the structure, and/or elemental composition of archaeological samples, obscuring differential diagnosis.

KEYWORDS

Bimbache, El Hierro, kidney stones, pre-Hispanic Canary Islands, SEM analysis, sesamoid bone, sialoliths, spherulites

This is an open access article under the terms of the [Creative Commons Attribution-NonCommercial-NoDerivs](https://creativecommons.org/licenses/by-nc-nd/4.0/) License, which permits use and distribution in any medium, provided the original work is properly cited, the use is non-commercial and no modifications or adaptations are made.

© 2023 The Authors. *Archaeometry* published by John Wiley & Sons Ltd on behalf of University of Oxford.

INTRODUCTION

Modern archaeological excavation techniques that include sieving the sediment around the skeletal remains and further microsedimentological analysis, allow the recovery of some minute calcified remains (Cárdenas-Arroyo & Martina, 2019). Identification of the exact nature of these structures constitutes a significant challenge because the list of minute and apparently mineral remains is very large. It includes seeds, remains of microfauna and microflora, sesamoid bones, kidney stones, gallstones or sialoliths (stones formed in the salivary ducts), and calcified lesions such as granuloma, myoma, phleboliths, atheromatous plaques, or pure mineral remains like spherulites, zeolites, or crystalline microaggregates (Verrecchia et al., 1995).

We have previously tested the ability of scanning electron microscopy (SEM) equipped with an energy-dispersive X-ray spectroscopy detector (EDX) to identify the composition and structure of these calcified remains. This approach enables identifying sesamoid bones, gallstones, sialoliths, and some stones formed in the urinary tract (González-Reimers et al., 2018; González-Reimers et al., 2020).

In the present study, we applied this methodology to analyze three different minute calcified structures recovered during the revisiting of a large collective pre-Hispanic burial from El Julán (El Hierro, Canary Islands). The re-excavation of this site was part of a project elaborated in 1994 to re-excavate and reanalyze burial caves that had been either excavated or spoiled in the past. Specifically, the burial cave from El Julán was explored since the end of the 19th century. At that time skeletal material was selectively collected, focusing on bones that served for osteometric and/or craniometric studies or those with striking pathological features (Verneau, 1879). During the re-excavation performed nearly 30 years ago, a few tiny calcified structures were additionally recovered.

As we have discussed, the possibility that the recovered minute remains correspond to actual organic material, such as biliary, urinary, or salivary calculi, is potentially useful for the reconstruction of the daily life of the pre-Hispanic people from El Hierro, given the information they can provide regarding diet and diseases suffered by these people.

Etiology, pathogenesis, and clinical significance of these remains are highly variable, as compiled by Steinbock (1989a, 1989b, 1990). For example, nonspecific, calcified granulomas may indicate many chronic infectious diseases such as tuberculosis or histoplasmosis (Kauffman, 2007). Aortic calcified atheromatous plaques (described by some of the authors in an old pre-Hispanic partially mummified woman from Gran Canaria [Martín-Herrera et al., 1987]) are markers of vascular risk (Duttaroy, 2021; Robertson & Strong, 1968). The rounded “mineral” structures could also correspond to gallstones, especially cholesterol gallstones, which may affect 10%–15% of people (Stinton & Shaffer, 2012), are related to obesity and women, and are also influenced by genetic factors, intestinal microbiome composition, and diet (Sun et al., 2022). Cholesterol gallstones are also associated with increased vascular risk (Sun et al., 2022). As other types of gallstones (black bilirubin gallstones, related to hemolytic anemia, or brownish colored gallstones related to bile duct infection by *Enterobacteriaceae*), they may cause potentially lethal diseases, such as pancreatitis or bile tract infection (Trotman, 1991).

Kidney stones are almost as frequent as gallstones, affecting about 9% of the Western population (Scales et al., 2012). This high frequency is related to different factors that alter urine composition, including the type of diet (Grases et al., 2006; Tebben et al., 2016) or acquired or genetic disorders affecting renal tubular transport of hydrogen ions and/or divalent cations (Edvardsson et al., 2013).

Urolithiasis may cause colicky pain and recurrent kidney infection, a potentially dangerous disease, even more so in the pre-antibiotic era (Eliakim-Raz et al., 2019). However, treatment-free survival after the first colicky episodes is possible, especially if the urine stream eliminates the stone. Eventually, nephrocalcinosis may complicate this clinical scenario and cause chronic

renal failure and end-stage renal disease, that is less common in calcium oxalate stone formers than in calcium phosphate stone formers (Bhojani et al., 2015).

Sialoliths or salivary stones are far less common. Dehydration, salivary gland infection, and saliva stagnation in the main salivary ducts may facilitate their development. It could also be produced by genetically conditioned mucin composition alterations (Schicht et al., 2021). Salivary gland infection is a definite risk if the salivary stream does not remove or eliminate the stone.

Sesamoid bones are also rounded, small, calcified structures that may be archaeologically recovered. The information that the finding of sesamoid bones can provide regarding lifestyle is uncertain but, as just commented, the identification of biliary, urinary, or salivary calculi, or other structures related to infection, vascular diseases, or parasites, is potentially useful for reconstructing the daily life of the pre-Hispanic people from El Hierro, given the information they can provide regarding diet and diseases. Therefore, in this study we applied the SEM/EDX technology to identify the composition and structure of tiny mineralized, roughly rounded structures with a diameter of less than 5 mm, recovered from a pre-Hispanic collective funerary cave from El Hierro (Canary Islands).

MATERIALS AND METHODS

Geographical and archaeological context

The island of El Hierro is the smallest (273 km²) and most recently formed of the seven islands of the Canarian Archipelago (Figure 1). The island has steep slopes up to 1500 m height over sea level. Volcanic eruptions gave origin to different landscapes. First, there are very rough, mainly basaltic *aa* lava flows that, given their relatively low inner temperature, partially solidified and broke into chaotic piles of irregular blocks now covering part of the island. There are also some vast *pahoehoe* fields, derived from a liquid lava stream at high temperature with a smooth surface that formed volcanic tubes of different sizes. On them, we can see the growth of scattered pines in the south and some small areas with dense forests in the northern cliffs and slopes, exposed to the humid Trade winds. The rest of the island is quite arid, partly due to its location at the southwestern corner of the archipelago. The climate is subtropical on the coast and dry in the south.

Before the Castilian conquest circa 1410, the island of El Hierro was inhabited by a pre-Hispanic population of Berber origin, known as Bimbaches (de la Jiménez Gómez, 1993). According to radiocarbon data compiled by Velasco Vázquez et al. (2019), they probably colonized the island around 1500–2000 years ago. Because the Island probably did not receive population arrivals after this first colonization until the Spanish conquest, isolation led to some kind of inbreeding, as shown by the genetic analysis of the remains of Punta Azul (Fregel et al., 2020; Ordóñez et al., 2017; Serrano et al., 2023). These studies have also identified mtDNA haplotypes similar to those observed among the pre-Hispanic population of all the Archipelago and North Africa (Fregel et al., 2019).

The pre-Hispanic individuals from collective burials in El Hierro were very robust, showing a normal-to-high trabecular bone mass, both in tibiae (Velasco-Vazquez et al., 1999) and in vertebrae (Gonzalez-Reimers et al., 2004). The stable carbon and nitrogen isotope analyses revealed the widespread and quantitatively important consumption of marine products (Arnay-de-la-Rosa et al., 2010), complemented by cereal consumption and some animal protein, probably from sheep and goats. These marine products can also be found in archaeological shell middens (de la Jiménez Gómez, 1993). The impact of isolation and low genetic diversity would explain the clustering of several cases of rare, genetically determined diseases, such as Klippel-Feil disease (González-Reimers et al., 2001).

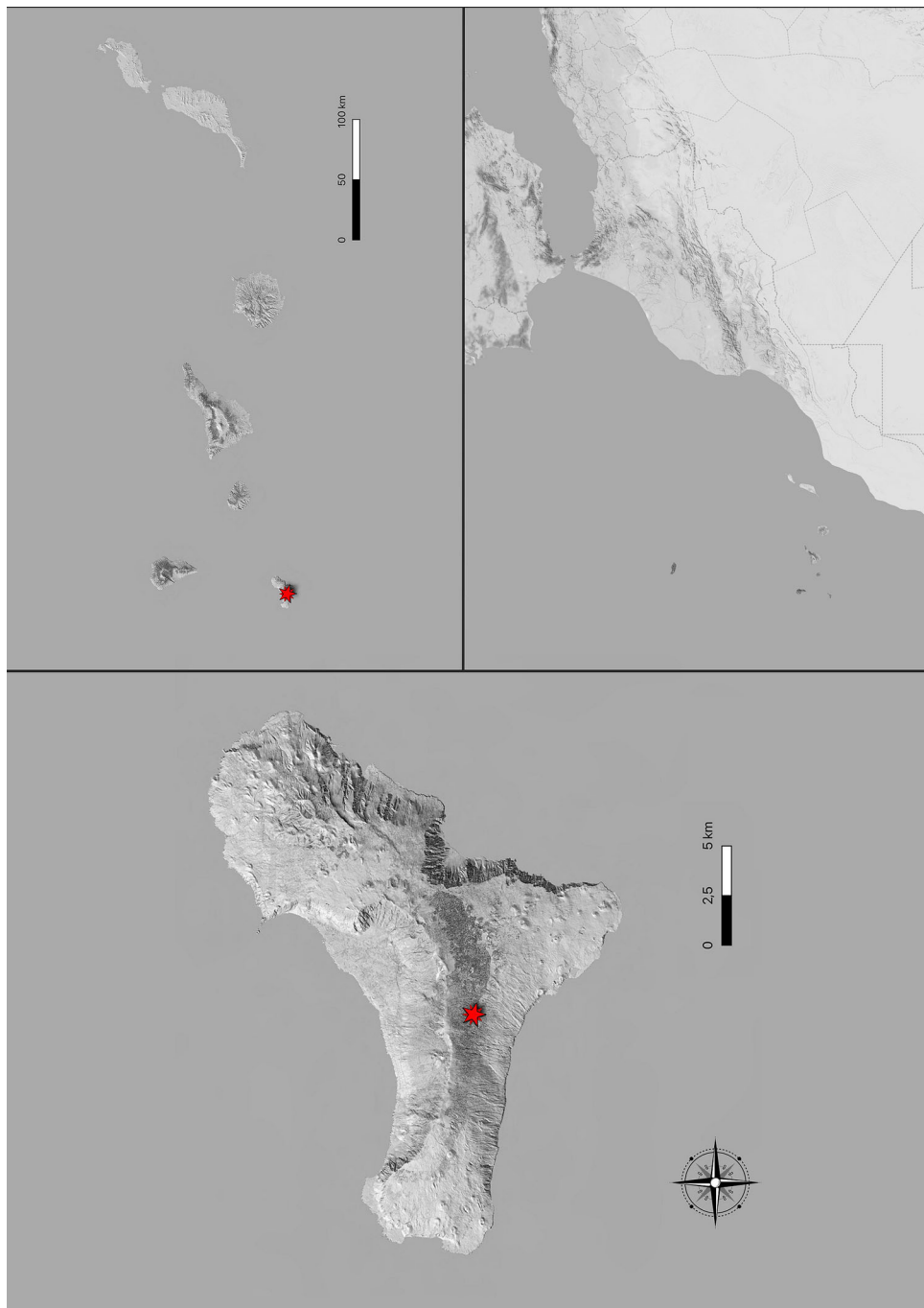


FIGURE 1 Location of the archaeological site of El Julán.

El Julán is the name given to an area of the Island's southern slopes (Figure 1). This area is profuse in archaeological remains of very different nature. We find panels of rock carvings, shell middens, dwelling remains, sacrificial altars containing remains of goatlings and lambs, archaeological sites presumed to be places where community councils took place, and several collective funerary caves (Hernández Pérez, 2002). Some of them were nearly completely spoiled, whereas others contained commingled remains. Under these circumstances, the burial caves of El Julán were included in the project of re-excavation of spoiled funerary sites.

In 1994, the burial caves of this area were grouped into two units. Unit 1 (Figure 2), located about 425 m above sea level, still preserved many skeletal fragments and contained remains of at least 38 human individuals. The remains corresponded to carpal, tarsal, splinters of other bones of hands and feet, parts of ribs, vertebrae, and three rounded calcified structures, initially recorded as sesamoid bones and/or possible calculi.

Samples

These three samples are roundly shaped with a relatively smooth outer surface. Sample 1 (Figure 3a) measured $11.5 \times 7 \times 9$ mm; Sample 2 (Figure 4a) measured $7.5 \times 4 \times 5$ mm and showed a small, disrupted area, and Sample 3 (Figure 5a) measured $5.5 \times 4 \times 2.8$ mm. and showed a more irregular surface. For comparative purposes, we also analyzed a small spherulite, measuring $14 \times 11 \times 10$ mm., found in southern Tenerife, with an outer appearance, shape, and size very similar to the analyzed samples (Figure 6a,b).



FIGURE 2 Plan of El Julán burial cave, with two images of the comingled remains. The squares with oblique lines correspond to the area excavated in 1994.

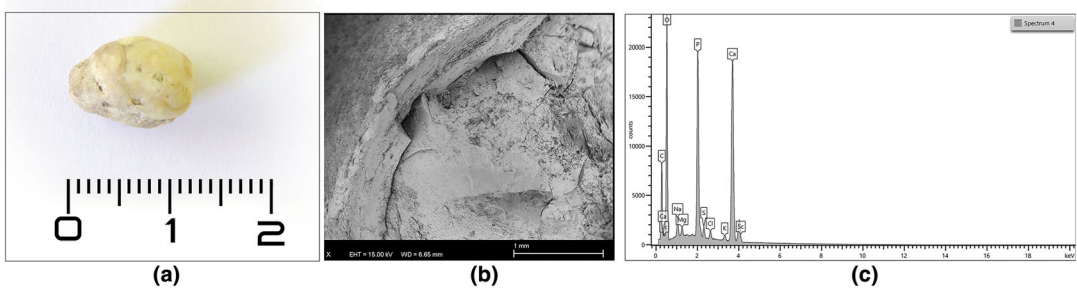


FIGURE 3 Sample 1, urolith. (a) Photograph of the sample with scale, outer aspect and measurements. (b) SEM image showing dense concentric layers compatible with a kidney stone. (c) Spectroscopic analysis. SE images.

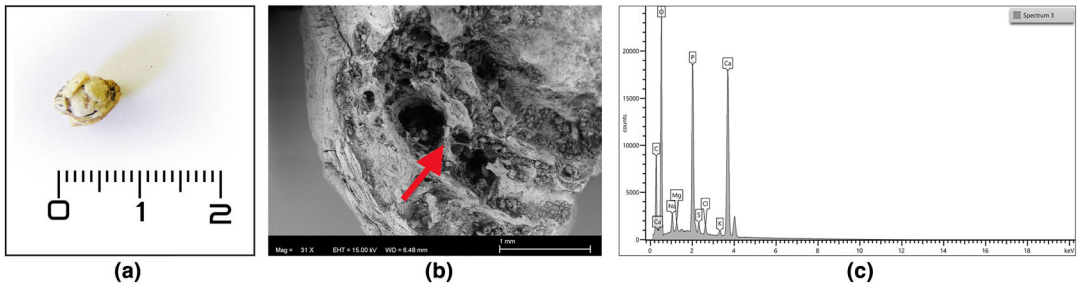


FIGURE 4 Sample 2, sesamoid. (a) Photograph of the sample with scale, outer aspect, and measurements. (b) SEM image showing bone trabeculae (signaled with a red arrow) surrounded by a relatively thin cortical shell. (c) Spectroscopic analysis. SE images.

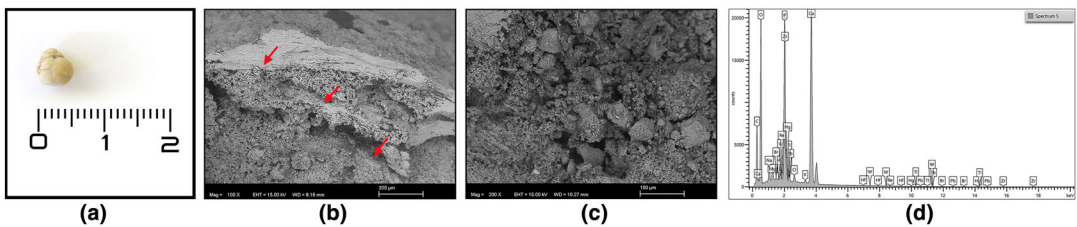


FIGURE 5 Sample 3, sialolith. (a) Photograph of the sample with scale, outer aspect and measurements. (b) SEM picture showing several concentric, laminated areas surrounding a core formed by loosely bound coarse grains. (c) Detail of the coarse grains located in the center. (d) Spectroscopic analysis. The three layers of the sialolith are marked with red arrows. SE images.

Sample analysis

First, the samples were gently brushed to remove dust. Second, they were mounted on an aluminum sample holder using adhesive carbon tape. They were analyzed in vacuum conditions (3.25×10^{-7} mbars), using a Zeiss EVO 15 (Zeiss, Oberkochen, Germany) scanning electron microscope (SEM) equipped with energy-dispersive X-ray spectroscopy (EDX) detector Oxford X-Max^N 80 mm² (Oxford instruments, High Wycombe, U.K.). This device is equipped with specific software able to identify (and quantify) the emission spectra of the different elements (with an atomic number >5) contained in the samples. We used an acceleration voltage of 20 keV, a working distance of 10 mm, and a probe current of 200 nA to get the best signal-to-noise ratio. The elemental analyses by EDX were made with a fixed acquisition of 300.000

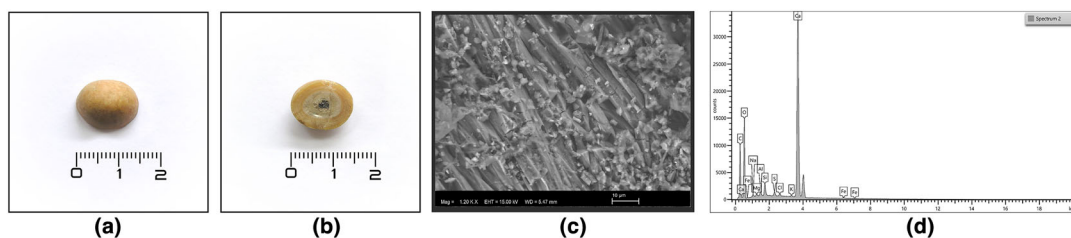


FIGURE 6 Spherulite, (a,b) Photograph of the sample with scale, showing outer aspect and measurements; SEM picture showing a crystalline structure (c). Spectroscopic analysis (d). SE images.

TABLE 1 Elemental composition of the samples, the spherulite, and the aluminum holder.

Element	Sample 1		Sample 2		Sample 3		Spherulite		Aluminum holder	
	Wt%	Atomic %	Wt%	Atomic %	Wt%	Atomic %	Wt%	Atomic %	Wt%	Atomic %
C	19.06	29.45	26.83	38.80	23.95	34.91	24.92	36.86	5.15	10.84
O	43.77	50.77	43.46	47.19	44.42	48.62	44.03	48.89	0.96	1.52
Na	1.18	0.96	-	-	1.38	1.05	0.36	0.28	-	-
Mg	0.85	0.65	-	-	0.88	0.63	0.22	0.16	0.72	0.74
Al	0.67	0.46	1.48	0.95	1.53	0.99	0.48	0.32	91.94	86.11
Si	1.68	1.11	-	-	4.32	2.69	0.98	0.62	0.55	0.50
P	10.28	6.16	6.47	3.63	6.50	3.68	-	-	-	-
S	0.72	0.42	-	-	0.68	0.37	0.35	0.20	-	-
Cl	0.46	0.24	-	-	0.69	0.34	0.24	0.12	-	-
K	0.82	0.39	-	-	0.95	0.42	0.15	0.07	-	-
Ca	19.73	9.14	21.75	9.43	13.50	5.90	27.91	12.37	-	-
Ti	-	-	-	-	0.24	0.09	-	-	-	-
Fe	0.77	0.26	-	-	0.97	0.30	0.34	0.11	0.34	0.15
Cu	-	-	-	-	-	-	-	-	0.34	0.14

counts for each spectrum. Afterward, we cut them around the midline with a lancet. SEM analyses were performed on the transverse sections to get highly detailed morphological information on different microscopic structures inside the samples. The SEM used for the analysis is an ESEM (environmental scanning electron microscope), which allows for the option of analyze specimens that are uncoated by allowing for a gaseous environment in the specimen chamber. Chamber pressure was adjusted to 10 Pa to eliminate charge disturbances.

EDX analyses were performed to get a mean global composition of the samples on a relatively wide area of the inner part of the samples, measuring $250 \times 150 \mu\text{m}$. For comparative purposes, the EDX composition of the aluminum holder was also assessed (Table 1). Based on the elemental composition of the samples, especially the Ca:P:O ratios, we inferred the presence of calcium phosphate and/or carbonate salts (Atkins & Jones, 1997).

RESULTS

SEM image of Sample 1 revealed it was composed of several concentric layers of a relatively compact material (Figure 3b). The spectroscopic analysis revealed the following atomic

composition (Figure 3c; Table 1): phosphorus 6.2%; calcium 9.1%; oxygen, 50.8%, and carbon, 29.5%. This composition is compatible with calcium phosphate ($(\text{PO}_4)_2 \text{Ca}_3$ (P:Ca:O = 2:3:8 \approx 6.2:9.1:25). The remaining oxygen (ap. 26%) and carbon (ap. 30%) could correspond to organic material. Therefore, one possibility is that they are amino acids. However, this proposition remains hypothetical because hydrogen (essential components of amino acids) cannot be detected by the described method due to its low atomic number, and nitrogen may overlap with neighbored elements such as carbon or oxygen.

Moreover, part of the carbon (10%–12%) might be contamination from the carbon tape used during the analysis (see Table 1).

SEM image of the disrupted area of Sample 2 allowed the identification of the bone trabeculae characteristic of cancellous bone (Figure 4b). The spectroscopic analysis revealed the following composition (Figure 4c; Table 1): calcium = 9.4%; phosphorus = 3.6%; oxygen = 47.2%, carbon = 38.8%. The above is compatible with hydroxyapatite ($\text{Ca}_5(\text{PO}_4)_3\text{OH}$), in which the relationships P:Ca:O are 3:5:13 (\approx 3.6:6:16). It might also contain some salts of calcium carbonate (CO_3Ca); (\approx 3:9:3). The remaining carbon (\approx 35%) and oxygen (\approx 22%) could correspond to collagen or any other organic material, such as nucleosides, or peptide chains. The C:O ratio is completely in the range of several peptides (containing, for instance, alanine + valine + methionine) or nucleosides (for instance, thymidine [Nelson et al., 2017]).

SEM image of sample three revealed that it is composed of several compact layers (Figure 5b) that surround a coarsely grained aggregate of different sizes of granules (Figure 5c). Elemental composition (Figure 5d) consisting of carbon (34.9%), phosphate (3.7%), calcium (5.9%), and oxygen (48.6%) but also small amounts of sulfur and other elements (Table 1). The proportions of P:Ca (0.62) resemble that of a recently analyzed sialolith corresponding to a modern individual (13.93:23.07 \approx 0.605; global mean of three measurements of the inner part of the sialolith = 0.623 [González-Reimers et al., 2020]).

The analysis of the spherulite revealed a crystalline structure (Figure 6c) and a composition compatible with calcium carbonate monohydrate ($\text{CO}_3\text{Ca H}_2\text{O}$; Table 1: 12.4% Ca; \approx 49% oxygen). As with the remaining samples, there is an excess of carbon, probably related to the carbon tape used in the procedure. However, some environmental contamination is also possible.

Table 1 shows the aluminum holder's elemental composition determined by EDX. As shown, 10.8% of carbon is detected, probably related to the adhesive carbon tape used.

DISCUSSION

The methodology proposed in this study allows us to identify the inner aspect and composition of the three samples. With this, we can now proceed to perform a differential diagnosis to try to establish the etiology of these remains. After doing so, we can discuss some of the implications of this identification in understanding some aspects of the Bimbache population. Furthermore, it will prove the usefulness of applying this method to archaeological remains.

a. Differential diagnosis

First, The SEM/EDX analysis of the spherulite clearly denotes its mineral nature; therefore, the diagnosis of this sample is straightforward.

The differential diagnosis of the remaining samples is very ample, and we have to consider location, size and outer shape, microscopic analysis, and chemical composition of the calcified remains we want to analyze. Rounded calcification may develop in the brain due to many illnesses, such as hypoparathyroidism (Mendes et al., 2018) or cysticercosis (Bustos & Coyle, 2020). In the thoracic cavity, we can find calcified atheromatous plaques derived from the thoracic aorta or calcified plaques corresponding to calcified pleuritis (Zhu et al., 2021).

Calcified granulomas also tend to develop in the lungs. Gallstones develop in the gallbladder, but calcified cysts caused by Echinococcosis usually affect the liver and are also located in the right upper abdominal quadrant (Matsunaga et al., 2020). Most urinary stones form in the kidneys or bladder, but phleboliths usually form in the pelvic veins (Luk et al., 2017), and enteroliths are in the bowel (Salelkar et al., 2011), that is, in a location similar to that in which urinary stones may be found. Other frequent abdominal calcified structures include calcified myoma (Hermida Pérez et al., 2003), pancreatic calcifications, or atheromatous plaques of the abdominal aorta. Finally, intraarticular or periarticular calcifications are located near the joints, and sesamoid bones are observed near fingers or toes.

Therefore, in an intact burial, the location of these structures, with respect to the skeleton, could provide clues to its origin. Unfortunately, in the cases presented here, the relative position of the described small structures is unknown and was indeed modified by taphonomic alterations and previous anthropogenic interventions. Accordingly, we had to perform the differential diagnosis without this crucial data.

According to the size and outer aspect of the calcified remains analyzed in this study, we can exclude many of the previously mentioned calcified structures. For example, calcified atheromatous plaques, or calcified hematoma walls, are not spheric and are usually much larger than the cases analyzed in this study (Kavčič et al., 2006). The sample's aspect is also incompatible with pleural calcifications, which are usually large plaques (Zhu et al., 2021). The samples morphology is also different from that of the tiny crusts, or the partially or calcified but empty cysts that surround some parasites, such as *Echinococcus*, *Dracunculus*, or *Paragonimiasis* (Yatera et al., 2015). Also, extensive calcifications of tumors, viscera, or the large coralliform renal calculi associated with recurrent kidney infections can be discarded (Romano et al., 2019). In addition, many forms of periarticular or intraarticular calcification related to gout, pseudogout, chondrocalcinosis, or other more uncommon conditions such as ochronosis (Van Offel et al., 1995) show a very different morphology from that of the structures reported here.

Many small calcified structures are rounded, apparently solid, and similar to our samples. Therefore, for a correct differential diagnosis, we needed a microscopic analysis, like the SEM and their chemical composition to identify them.

One of the first elements to consider is the presence of trabeculae, as it strongly implies the existence of bone tissue in the calcified remains. These structures may correspond to sesamoid bones, although theoretically, some trabeculae could also be identified in some cases of osteochondritis dissecans (OD) (Jones & Williams, 2016). In this disease, a part of the articular cartilage breaks and floats freely into the synovial fluid (Bruns et al., 2018). The detached cartilage's outer cells can extract nutrients and survive in this fluid, but the central cells usually die and become calcified, forming a compact structure. However, some subchondral bone (attached to the cartilage) may sometimes break with the cartilage. Hence, some trabeculae could be theoretically identifiable in these cases (Uozumi et al., 2009). In addition, bone cysts may develop in the detached subchondral bone, posing difficulties in interpreting the SEM images, especially when dealing with dry osseous material in ancient samples, as is our case. OD is a common entity in the modern population and may be observed in several joints, especially knees, ankles, and elbows. The disease is divided into juvenile and adult forms, and is frequently observed among sportsmen. Interestingly, the type of sport might be related to the development of osteochondritis in certain joints (for instance, football and basketball are associated with knee or talar OD, whereas throwing athletes tend to develop OD in the elbows). A genetic predisposition also exists (Chau et al., 2021), and the exact incidence is not known, although the figures range from 2.3–31.6/100.000/year (Turati et al., 2023), and also has a high prevalence in modern populations (15–29/100.000 (Bruns et al., 2018)). Given the main economic activity as goat or shepherders of the pre-Hispanic inhabitants of El Hierro, OD was also likely a common disease among this population. In the compilation published by Zúñiga Thayer et al. (2018), some authors have reported very high frequencies of osteochondritis dissecans (ranging from 0.8% to

42.3%) in past populations. However, the prevalence of sesamoid bones is by far higher, affecting around 50% of the population (Yammine, 2014). The SEM image of sample 2 reported in this manuscript (Figure 4b) clearly shows trabeculae. Its composition fits well with bone hydroxyapatite ($\text{Ca}_5(\text{PO}_4)_3\text{OH}$), although there are calcium phosphate salts in many calcified structures (Murungi et al., 2004). Considering the results of SEM/EDX analysis, the higher prevalence of sesamoid bone, and the fact that the presence of trabeculae in OD is a rare phenomenon, we can conclude that Sample 2 is most likely a sesamoid bone.

The precise identification of the remaining two samples is more complicated. Case Number 1 strongly suggests a kidney stone. These stones show quite a variable composition with different clinical meanings. Urine is a fluid containing several substances in a metastable equilibrium at supersaturated levels so that they can either crystallize or remain as solutes, depending on urinary pH and variations in solute concentrations. Dietary habits may alter this equilibrium. The most frequently observed urinary calculi are those composed of calcium salts. In general, alkaline urine ($\text{pH} > 6$) favors the formation of calcium-containing crystals, as has been observed in individuals consuming a mainly vegetarian diet, whereas acid urine ($\text{pH} < 5$), associated, for instance, with a high protein diet, may cause oxalate and uric acid deposition. Calcium-containing nephroliths may also be related to diets with excessive calcium or vitamin D intake (Tebben et al., 2016).

Some genetic disorders that could lead to calculi formation, like Type 1 Hyperoxaluria and idiopathic hypercalciuria show an abnormally high prevalence among the current population of some Canarian Islands, like La Gomera (García-Nieto et al., 2020), and have also been commonly described in Tunisia (Nagara et al., 2013). Therefore, they should be included in the differential diagnosis.

Other rare causes of calcified uroliths are related to other major causes of hypercalcemia, such as malignancy, hyperparathyroidism, or granulomatous diseases (Turner, 2017).

Malabsorptive conditions, especially those associated with fat malabsorption, such as inflammatory bowel disease, may paradoxically increase enteric oxalate absorption and cause hyperoxaluria and calcium oxalate kidney stones (Dobbins & Binder, 1976).

Dietary habits also cause other types of kidney stones. Excessive purine intake, which can come from excessive meat or seafood intake, together with acid urine output, may provoke uric acid kidney stones (Abou-Elela, 2017). This happens especially when combined with disorders of uric acid excretion.

Kidney infection may lead to the formation of struvite stones that contain magnesium salts, although their composition becomes altered after exposure to environmental factors (Williams et al., 2012). There are other less common causes of urolithiasis (Grases et al., 2006). Eventually, nephrocalcinosis may complicate this clinical scenario and cause chronic renal failure and an end-stage renal disease, which is less common in calcium oxalate stone formers than in calcium phosphate stone formers (Bhojani et al., 2015).

The most frequently observed kidney stones include those formed by calcium phosphate salts (whewellite, Nilsson Stutz, 2021) or dihydrate (weddellite), uric acid stones and struvite (magnesium ammonium phosphate), and others of relatively uncommon composition (Steinbock, 1989b). Their size is variable, usually between 10 and 20 mm, although many of them range between 1 and 2 mm and a few over 5–6 cm (Fakhr Yasseri et al., 2021; Kalathia et al., 2021). However, in most instances, they fit in shape and size with the sample presented here (Shah & Calle, 2016). Although the chemical composition is like that of a bone, perhaps with a slightly higher Ca/P ratio, the lack of a bony structure (Figure 4) supports the identification of Sample 1 as a urolith. The presence of small amounts of other elements in the EDX spectrum that do not correspond to organic animal structures, such as silicon, aluminum, sodium, iron, sulfur, or even magnesium, is very likely due to contamination from a soil derived from mafic lava eruptions. Nevertheless, their presence in such amounts will not disturb the correct interpretation of the composition of the calcified structure. In this sense, the elemental

composition of this sample is compatible with that of a kidney stone, although a calcified granuloma cannot be easily discarded. However, they are usually less compact than uroliths as they are a group of transformed macrophages and fibroblasts that become surrounded by calcium salts.

The composition of Sample 3 could also be compatible with a kidney stone (Ventura et al., 2022). Nevertheless, the fine-grained aspect of its inner part, not typical of these structures, has led us to propose it could be a sialolith.

Kraaij et al. (2018) thoroughly analyzed the structure of sialoliths, related to their pathogenesis. The initial agglomeration of desquamated epithelial cells, mucin, or bacteria becomes packed together by calcium phosphate salts and is ultimately surrounded by laminated organic and inorganic material layers. Further deposition of these microaggregates and the formation of new laminated layers surrounding them form a final structure consisting of alternating microaggregates (Figure 5c) and more compact layers (Figure 5b), similar to that reported for sialoliths affecting modern individuals (Busso et al., 2020; González-Reimers et al., 2020). Therefore, the SEM image of Sample 3 would be compatible with a sialolith.

The composition of this sample also matches the one reported for sialoliths, but it does not allow clear-cut discrimination with that of a kidney stone. The P:Ca proportion (0.62) is very similar to those of recently analyzed clinical sialoliths cases (González-Reimers et al., 2020) and to the values reported by other authors (Pellegrino & Biltz, 1968) P:Ca atomic ratio = 0.598; Stelmach et al. (2016) P:Ca = 3:5 (0.60). Small amounts of magnesium, related with the deposition of small amounts of whitlockite, have also been described in some modern sialoliths (Teymoortash et al., 2003). Similarly, small amounts of sulfur (Stelmach et al., 2016) could correspond to sulfur-rich amino acids such as cysteine (Nelson et al., 2017). In this sense, sulfur-containing bacteria are usual in patients affected by periodontitis (Tsai et al., 2008), and there is an association between sialolithiasis and periodontal disease (Hung et al., 2016). However, we cannot exclude that, in this case, some contamination with soil components rich in sulfur or magnesium could have contributed to the obtained results. This would also be the case with the tiny amounts of chlorine, titanium, or other elements shown in the results. The background noise of the EDX measurement could also be responsible for these elements' presence. Consequently, both the SEM image and composition analysis of Sample 3 are compatible with a sialolith. Despite its similar composition to Sample 1, the fine-grained structure between the concentric layers, the Ca:P ratio, and the presence of sulfur suggest that we are dealing with a sialolith.

In summary, organic mineralized structures formed by human beings recovered during archaeological burial excavations can contain calcium phosphate salts, and smaller amounts of calcium carbonate and calcium/magnesium carbonate, with or without traces of other elements. Therefore, it is very difficult to properly differentiate bony structures, calcified calculi, or granuloma based solely on chemical criteria (Dorozhkin, 2012), but SEM (or macroscopic) images are useful tools for this purpose. For instance, bone trabeculae are absent from calculi. In addition, studies on calcified granuloma or other kinds of calcification present images that strongly differ from those of the calculi analyzed here (Colboc et al., 2016). In any case, EDX constitutes a valuable tool to differentiate calcified organic structures from aragonite spherulites, zeolites, or iron oxide nodules that can be recovered during modern burial excavations and initially misinterpreted as calcified organic remains.

b. Archaeological/anthropological considerations

This research supports the usefulness of SEM analysis in identifying tiny 'mineral' remains recovered while excavating a burial site, an important step in interpreting the archaeological significance of these findings.

As already mentioned, in Case Number 2, there is little doubt that it corresponds to a sesamoid bone. Hand or feet sesamoid bones are small rounded or oval-shaped bones located, in variable numbers, usually around the metacarpal/metatarsal-phalangeal joints. They are formed by a central part of cancellous bone and a thin cortex, as clearly observable in the case's SEM picture. Sesamoid bones are very common, especially in some anatomical regions. Nearly everybody has one or two sesamoid bones at the first metacarpophalangeal joint (Dąbrowski et al., 2019). In addition, the number of sesamoid bones located in places other than the first metacarpophalangeal joint differs among different population groups, suggesting that genetics could play a role in their development (Chen et al., 2015). It has been speculated that their presence can be related to mechanical stress (Berthaume et al., 2019). The problem in establishing this relationship in prehistoric populations resides in the fact that their presence in burial excavations is not frequently reported, and we cannot be sure if their paucity or absence really indicates a low prevalence, or if it is simply due to unawareness of their presence. In this burial excavation, we cannot be sure that all the sesamoid bones were recovered, so we cannot infer any conclusion based on their prevalence among the pre-Hispanic population from El Hierro.

In the case of kidney stones, they affect about 9% of the Western population (Scales et al., 2012), and calcium-containing stones are the most frequently observed. Therefore, the finding of this kind of stones among the pre-Hispanic population of the Canary Islands may bear an additional interest. Furthermore, as previously commented, the formation of some calcium-containing kidney stones is genetically determined. Among them, primary hyperoxaluria shows a prevalence of 1–3 per million people (Edvardsson et al., 2013). Nonetheless, in the modern population of the Canary Islands, the prevalence is far higher, especially in places like La Gomera or Tunisia (García-Nieto et al., 2020; Nagara et al., 2013). In addition, genetic studies have revealed that the pre-Hispanic population of the Canary Islands was strongly related to the North African Berbers (Fregel et al., 2019), and many haplotypes found in the pre-Hispanic population are frequently detected in the modern population of the islands, especially in La Gomera (Fregel et al., 2019). Therefore, the hypothesis of an inherited genetic risk for idiopathic hyperoxaluria and/or idiopathic hypercalciuria should be considered. However, establishing the prevalence of kidney stones among the pre-Hispanic population is still problematic.

Another possibility to be considered for explaining the presence of these stones is the influence of dietary patterns (Grases et al., 2006; Tebben et al., 2016). Paleodietary studies on the pre-Hispanic population of El Hierro point to the consumption of marine products, although cereal consumption was also widespread (Arnay-de-la-Rosa et al., 2010). Nevertheless, we cannot be sure that all the kidney stones were recovered. Therefore, one case may constitute an anecdotal finding not related to a genetic penetrance of Type I hyperoxaluria or idiopathic hypercalciuria or to a generalized consumption of a vegetarian diet.

In the case of Sample 3 implications, we must consider that sialoliths are uncommon. Factors predisposing to their development are poorly known, but they may include dehydration and periodontitis (Duong et al., 2019). They may also be associated with Sjögren disease (Konstantinidis et al., 2007). Spontaneous elimination of a salivary stone is more complicated than that of kidney stones. A persistent stone in the salivary gland or ducts usually leads to sialadenitis, a very painful and dangerous disease in the pre-antibiotic era.

CONCLUSIONS

As said, this research supports the usefulness of SEM analysis in identifying tiny 'mineral' remains recovered during an archaeological excavation. However, some issues should be considered.

When we compare the outer aspect of the three archaeological samples and that of the spherulite, little differences can be observed because uroliths, sialoliths, sesamoid bones, spherulites, or more or less calcified seeds show a similar shape and aspect to the bare eye. Therefore, only the outer aspect of all these tiny structures may provide little help in their proper identification. Hence, as this study shows, SEM/EDX technology constitutes a valuable tool for the study of this category of remains.

In some cases, the presence of trabeculae is virtually diagnostic. Still, in other cases, the SEM aspect may be less specific or nonspecific at all. Additionally, a pure chemical analysis may be misleading because many organic calcified structures contain calcium phosphate salts as their primary component and soil contamination may obscure a correct interpretation. Hence, we believe that combining both methods is crucial to correctly identify these remains. SEM analysis with EDX clearly serves to identify sesamoid bones or crystalline mineral structures, but its role in the differential diagnosis of different calculi may be more controversial. More reports of this kind of studies on archaeological material are needed, especially considering the influence of soil characteristics and taphonomic processes that may have altered the structure and composition of any organic calcified structure. Indeed, detailed comparative analysis of the elemental composition and morphological aspect, both of non-altered modern samples and antique ones, require further research.

ACKNOWLEDGEMENTS

The first author is funded by “Contratos postdoctorales para la especialización de personal investigador, convocatoria 2020, ULPGC.”

PEER REVIEW

The peer review history for this article is available at <https://www.webofscience.com/api/gateway/wos/peer-review/10.1111/arcm.12934>.

DATA AVAILABILITY STATEMENT

The data that support the findings of this study are all included in this article.

ORCID

Alejandra C. Ordóñez  <https://orcid.org/0000-0003-3568-3246>

REFERENCES

- Abou-Elela, A. (2017). Epidemiology, pathophysiology, and management of uric acid urolithiasis: A narrative review. *Journal of Advanced Research*, 8(5), 513–527. <https://doi.org/10.1016/j.jare.2017.04.005>
- Arnay-de-la-Rosa, M., González-Reimers, E., Yanes, Y., Velasco-Vázquez, J., Romanek, C. S., & Noakes, J. E. (2010). Paleodietary analysis of the prehistoric population of the Canary Islands inferred from stable isotopes (carbon, nitrogen and hydrogen) in bone collagen. *Journal of Archaeological Science*, 37(7), 1490–1501. <https://doi.org/10.1016/j.jas.2010.01.009>
- Atkins, P. W., & Jones, L. L. (1997). *Chemistry: Molecules, matter, and change* (3rd ed.). W. H Freeman.
- Berthaume, M. A., Di Federico, E., & Bull, A. M. J. (2019). Fabella prevalence rate increases over 150 years, and rates of other sesamoid bones remain constant: A systematic review. *Journal of Anatomy*, 235(1), 67–79. <https://doi.org/10.1111/joa.12994>
- Bhojani, N., Paonessa, J. E., Hameed, T. A., Worcester, E. M., Evan, A. P., Coe, F. L., Borofsky, M. S., & Lingeman, J. E. (2015). Nephrocalcinosis in calcium stone formers who do not have systemic disease. *Journal of Urology*, 194(5), 1308–1312. <https://doi.org/10.1016/j.juro.2015.05.074>
- Bruns, J., Werner, M., & Habermann, C. (2018). Osteochondritis dissecans: Etiology, pathology, and imaging with a special focus on the knee joint. *Cartilage*, 9(4), 346–362. <https://doi.org/10.1177/1947603517715736>
- Busso, C. S., Guidry, J. J., Gonzalez, J. J., Zorba, V., Son, L. S., Winsauer, P. J., & Walvekar, R. R. (2020). A comprehensive analysis of sialolith proteins and the clinical implications. *Clinical Proteomics*, 17(1), 12. <https://doi.org/10.1186/s12014-020-09275-w>
- Bustos, J. A., & Coyle, C. M. (2020). Brain calcification because of neurocysticercosis: A vast field to be explored. *Current Opinion in Infectious Diseases*, 33(5), 334–338. <https://doi.org/10.1097/QCO.0000000000000673>

- Cárdenas-Arroyo, F., & Martina, M. C. (2019). Two findings of gallstones in archaeological mummies from Colombia. *International Journal of Paleopathology*, 24, 53–59. <https://doi.org/10.1016/j.ijpp.2018.09.003>
- Chau, M. M., Klimstra, M. A., Wise, K. L., Ellermann, J. M., Tóth, F., Carlson, C. S., Nelson, B. J., & Tompkins, M. A. (2021). Osteochondritis dissecans: Current understanding of epidemiology, etiology, management, and outcomes. *Journal of Bone and Joint Surgery. American*, 103(12), 1132–1151. <https://doi.org/10.2106/JBJS.20.01399>
- Chen, W., Cheng, J., Sun, R., Zhang, Z., Zhu, Y., Ipaktchi, K., & Zhang, Y. (2015). Prevalence and variation of sesamoid bones in the hand: A multi-center radiographic study. *International Journal of Clinical and Experimental Medicine*, 8(7), 11721–11726.
- Colboc, H., Bazin, D., Moguelet, P., Frochot, V., Weil, R., Letavernier, E., Jouanneau, C., Francès, C., Bachmeyer, C., Bernaudin, J.-F., & Daudon, M. (2016). Detection of silica and calcium carbonate deposits in granulomatous areas of skin sarcoidosis by μ Fourier transform infrared spectroscopy and field emission scanning electron microscopy coupled with energy dispersive X-ray spectroscopy analysis. *From Urolithiasis to Pathological Calcifications*, 19(11), 1631–1641. <https://doi.org/10.1016/j.crci.2016.05.007>
- Dąbrowski, K., Stankiewicz-Jóźwicka, H., Kowalczyk, A., Markuszewski, M., & Ciszek, B. (2019). Ossa Sesamoidea—prevalence of sesamoid bones in human hands. *Folia Morphologica*, 79, 570–575. <https://doi.org/10.5603/FM.a2019.0123>
- de la Jiménez Gómez, M. C. (1993). *El Hierro y los Bimbaches*. Centro de la Cultura Popular Canaria.
- Dobbins, J. W., & Binder, H. J. (1976). Effect of bile salts and fatty acids on the colonic absorption of oxalate. *Gastroenterology*, 70(6), 1096–1100. [https://doi.org/10.1016/S0016-5085\(76\)80318-6](https://doi.org/10.1016/S0016-5085(76)80318-6)
- Dorozhkin, S. V. (2012). Calcium orthophosphates and human beings: A historical perspective from the 1770s until 1940. *Biomater*, 2(2), 53–70. <https://doi.org/10.4161/biom.21340>
- Duong, L. T., Kakiche, T., Ferré, F., Nawrocki, L., & Bouattour, A. (2019). Management of anterior submandibular sialolithiasis. *Journal of Oral Medicine and Oral Surgery*, 25(2), 16. <https://doi.org/10.1051/mbcb/2018039>
- Duttaroy, A. K. (2021). Role of gut microbiota and their metabolites on atherosclerosis, hypertension and human blood platelet function: A review. *Nutrients*, 13(1), 144. <https://doi.org/10.3390/nu13010144>
- Edvardsson, V. O., Goldfarb, D. S., Lieske, J. C., Beara-Lasic, L., Anglani, F., Milliner, D. S., & Palsson, R. (2013). Hereditary causes of kidney stones and chronic kidney disease. *Pediatric Nephrology (Berlin, Germany)*, 28(10), 1923–1942. <https://doi.org/10.1007/s00467-012-2329-z>
- Eliakim-Raz, N., Babitch, T., Shaw, E., Addy, I., Wiegand, I., Vank, C., Torre-Vallejo, L., Joan-Miquel, V., Steve, M., Grier, S., Stoddart, M., Nienke, C., van den Leo, H., Vuong, C., MacGowan, A., Carratalà, J., Leibovici, L., & Pujol, M. (2019). Risk factors for treatment failure and mortality among hospitalized patients with complicated urinary tract infection: A multicenter retrospective cohort study (rescuing study group). *Clinical Infectious Diseases: An Official Publication of the Infectious Diseases Society of America*, 68(1), 29–36. <https://doi.org/10.1093/cid/ciy418>
- Fakhr Yasser, A., Saatchi, M., Khatami, F., Dialameh, H., Rahimzadeh, H., & Aghamir, S. M. K. (2021). The prevalence of renal stones and outcomes of conservative treatment in kidney transplantation: A systematic review and Meta-analysis. *Urology Journal*, 18(3), 252–258. <https://doi.org/10.22037/uj.v18i02.6531>
- Fregel, R., Ordóñez, A. C., Santana-Cabrera, J., Cabrera, V. M., Velasco-Vázquez, J., Alberto, V., Moreno-Benitez, M. A., Delgado-Darias, T., Rodríguez-Rodríguez, A., Hernández, J. C., Pais, J., González-Montelongo, R., Lorenzo-Salazar, J. M., Flores, C., Cruz-de-Mercadal, M. C., Álvarez-Rodríguez, N., Shapiro, B., Arnay, M., & Bustamante, C. D. (2019). Mitogenomes illuminate the origin and migration patterns of the indigenous people of the Canary Islands. *PLoS ONE*, 14(3), e0209125. <https://doi.org/10.1371/journal.pone.0209125>
- Fregel, R., Ordóñez, A. C., & Serrano, J. G. (2020). The demography of the Canary Islands from a genetic perspective. *Human Molecular Genetics*, 30(R1), R64–R71. <https://doi.org/10.1093/hmg/ddaa262>
- García-Nieto, V. M., Claverie-Martín, F., Perdomo-Ramírez, A., Cárdoaba-Lanus, E., Ramos-Trujillo, E., Mura-Escorche, G., Tejera-Carreño, P., & Luis-Yanes, M. I. (2020). Consideraciones acerca de las bases moleculares de algunas tubulopatías en relación con la endogamia y los desplazamientos poblacionales. *Nefrología*, 40(2), 126–132. <https://doi.org/10.1016/j.nefro.2019.08.004>
- González-Reimers, E., Frías-García, M., & Arnay-de-la-Rosa, M. (2020). Identifying sialoliths through SEM technology. *International Journal of Paleopathology*, 31, 60–63. <https://doi.org/10.1016/j.ijpp.2020.10.004>
- González-Reimers, E., González-Arnay, E., Castañeyra-Ruiz, M., & Arnay-de-la-Rosa, M. (2018). Identifying small pelvic inclusions through SEM technology. *International Journal of Paleopathology*, 22, 92–96. <https://doi.org/10.1016/j.ijpp.2018.06.003>
- González-Reimers, E., Mas-Pascual, A., Arnay-de-la-Rosa, M., Velasco-Vázquez, J., & Jiménez-Gómez, M. C. (2001). Klippel-Feil syndrome in the prehispanic population of El Hierro (Canary Islands). *Annals of the Rheumatic Diseases*, 60(2), 173–177. <https://doi.org/10.1136/ard.60.2.173a>
- Gonzalez-Reimers, E., Mas-Pascual, M. A., Arnay-de-la-Rosa, M., Velasco-Vazquez, J., Santolaria-Fernandez, F., & Machado-Calvo, M. (2004). Noninvasive estimation of bone mass in ancient vertebrae. *American Journal of Physical Anthropology*, 125(2), 121–131. <https://doi.org/10.1002/ajpa.10374>

- Grases, F., Costa-Bauza, A., & Prieto, R. M. (2006). Renal lithiasis and nutrition. *Nutrition Journal*, 5(1), 23. <https://doi.org/10.1186/1475-2891-5-23>
- Hermida Pérez, J., Vento Remedios, T., Ramos Pérez, A., Guerra Abrante, P., & Ochoa Urdangarain, O. (2003). *Mioma uterino calcificado*. Presentación de tres casos. Archivos Españoles de Urología.
- Hernández Pérez, M. (2002). *El Julán (La Frontera, El Hierro, Islas Canarias)*, Gobierno de Canarias. Dirección General de Patrimonio Histórico, Canarias.
- Hung, S.-H., Huang, H.-M., Lee, H.-C., Ching Lin, H., Kao, L.-T., & Wu, C.-S. (2016). A population-based study on the association between chronic periodontitis and sialolithiasis. *Laryngoscope*, 126(4), 847–850. <https://doi.org/10.1002/lary.25360>
- Jones, M. H., & Williams, A. M. (2016). Osteochondritis dissecans of the knee: A practical guide for surgeons. *Bone & Joint Journal*, 98-B(6), 723–729. <https://doi.org/10.1302/0301-620X.98B6.36816>
- Kalathia, J., Patel, K., & Agrawal, S. (2021). Giant prostatic and bladder calculi: Endoscopic management and review of the literature. *Urology Case Reports*, 35, 101529. <https://doi.org/10.1016/j.eucr.2020.101529>
- Kauffman, C. A. (2007). Histoplasmosis: A clinical and laboratory update. *Clinical Microbiology Reviews*, 20(1), 115–132. <https://doi.org/10.1128/CMR.00027-06>
- Kavčič, A., Meglič, B., Meglič, P., Vodusek, D. B., & Mesec, D. (2006). Asymptomatic huge calcified subdural hematoma in a patient on oral anticoagulant therapy. *Neurology*, 66(5), 758. <https://doi.org/10.1212/01.wnl.0000200960.84140.d9>
- Konstantinidis, I., Paschaloudi, S., Triaridis, S., Fyrmpas, G., Sechlidis, S., & Constantinidis, J. (2007). Bilateral multiple sialolithiasis of the parotid gland in a patient with Sjögren's syndrome. *Acta Otorhinolaryngologica Italica: Organo Ufficiale Della Società Italiana di Otorinolaringologia e Chirurgia Cervico-Facciale*, 27(1), 41–44.
- Kraaij, S., Brand, H.-S., van der Meij, E.-H., & de Visscher, J.-G. (2018). Biochemical composition of salivary stones in relation to stone- and patient-related factors. *Medicina Oral, Patologia Oral Y Cirugia Bucal*, 23(5), e540–e544. <https://doi.org/10.4317/medoral.22533>
- Luk, A. C. O., Cleaveland, P., Olson, L., Neilson, D., & Srirangam, S. J. (2017). Pelvic phlebolith: A trivial pursuit for the urologist? *Journal of Endourology*, 31(4), 342–347. <https://doi.org/10.1089/end.2016.0861>
- Martin-Herrera, A., Arnay-da-la-Rosa, M., González-Reimers, E., Jorge-Hernández, J. A., & Díaz-Flores, L. (1987). Histological observations in a pre-Hispanic mummy of Gran Canaria. *Journal of Paleopathology*, 1, 33–36.
- Matsunaga, Y., Ariizumi, S., Shibuya, G., Uemura, S., Kato, T., Yazawa, T., Yamashita, S., Omori, A., Higuchi, R., Takahashi, Y., Kotera, Y., Egawa, H., & Yamamoto, M. (2020). Hepatocellular carcinoma with ring calcification mimicking hydatid disease: A case report. *Surgical Case Reports*, 6(1), 171. <https://doi.org/10.1186/s40792-020-00927-5>
- Mendes, E. M., Meireles-Brandão, L., Meira, C., Morais, N., Ribeiro, C., & Guerra, D. (2018). Primary hypoparathyroidism presenting as basal ganglia calcification secondary to extreme hypocalcemia. *Clinics and Practice*, 8(1), 1007. <https://doi.org/10.4081/cp.2018.1007>
- Murungi, J. I., Thiam, S., Tracy, R. E., Robinson, J. W., & Warner, I. M. (2004). Elemental analysis of soft plaque and calcified plaque deposits from human coronary arteries and aorta. *Journal of Environmental Science and Health. Part a, Toxic/Hazardous Substances & Environmental Engineering*, 39(6), 1487–1496. <https://doi.org/10.1081/ESE-120037848>
- Nagara, M., Tiar, A., Ben Halim, N., Ben Rhouma, F., Messaoud, O., Bouyacoub, Y., Kefi, R., Hassayoun, S., Zouari, N., Ben Ammar, M. S., Abdelhak, S., & Chemli, J. (2013). Mutation spectrum of primary hyperoxaluria type 1 in Tunisia: Implication for diagnosis in North Africa. *Gene*, 527(1), 316–320. <https://doi.org/10.1016/j.gene.2013.06.023>
- Nelson, D. L., Cox, M. M., & Lehninger, A. L. (2017). *Lehninger Principles of Biochemistry*.
- Nilsson Stutz, L. (2021). Building bridges between burial archaeology and the archaeology of death—Where is the archaeological study of the dead going. *Current Swedish Archaeology*, 26, 13–35. <https://doi.org/10.37718/CSA.2016.01>
- Ordóñez, A. C., Fregel, R., Trujillo-Mederos, A., Hervella, M., de-la-Rúa, C., & Arnay-de-la-Rosa, M. (2017). Genetic studies on the prehispanic population buried in Punta Azul cave (El Hierro, Canary Islands). *Journal of Archaeological Science*, 78, 20–28. <https://doi.org/10.1016/j.jas.2016.11.004>
- Pellegrino, E. D., & Biltz, R. M. (1968). Bone carbonate and the Ca to P molar ratio. *Nature*, 219(5160), 1261–1262. <https://doi.org/10.1038/2191261a0>
- Robertson, W. B., & Strong, J. P. (1968). Atherosclerosis in persons with hypertension and diabetes mellitus. *Laboratory Investigation: A Journal of Technical Methods and Pathology*, 18(5), 538–551.
- Romano, J., Estrada, C., & Suárez, N. (2019). Litiasis coraliforme. *Atención Primaria*, 51(7), 452–453. <https://doi.org/10.1016/j.aprim.2018.09.014>
- Salelkar, R. S., Patil, R. T., Amonkar, D. P., & Sardesai, S. G. (2011). Enterolith with enterocolic fistula: The diagnostic approach. *Saudi Journal of Gastroenterology: Official Journal of the Saudi Gastroenterology Association*, 17(6), 418–420. <https://doi.org/10.4103/1319-3767.87186>
- Scales, C. D. J., Smith, A. C., Hanley, J. M., & Saigal, C. S. (2012). Prevalence of kidney stones in the United States. *European Urology*, 62(1), 160–165. <https://doi.org/10.1016/j.eururo.2012.03.052>

- Schicht, M., Reichle, A., Schapher, M., Garreis, F., Kleinsasser, B., Aydin, M., Sahin, A., Iro, H., & Paulsen, F. (2021). The translational role of MUC8 in salivary glands: A potential biomarker for salivary stone disease? *Diagnosics (Basel, Switzerland)*, 11(12), 2330. <https://doi.org/10.3390/diagnostics11122330>
- Serrano, J. G., Ordóñez, A. C., Santana, J., Sánchez-Cañadillas, E., Arnay, M., Rodríguez-Rodríguez, A., Morales, J., Velasco-Vázquez, J., Alberto-Barroso, V., Delgado-Darias, T., de Mercadal, M. C. C., Hernández, J. C., Moreno-Benitez, M. A., Pais, J., Ringbauer, H., Sikora, M., McColl, H., Pino-Yanes, M., Ferrer, M. H., Bustamante, C. D., & Fregel, R. (2023). The genomic history of the indigenous people of the Canary Islands. *Nature Communications*, 14(1), 4641. <https://doi.org/10.1038/s41467-023-40198-w>
- Shah, S., & Calle, J. C. (2016). Dietary and medical management of recurrent nephrolithiasis. *Cleveland Clinic Journal of Medicine*, 83(6), 463–471. <https://doi.org/10.3949/ccjm.83a.15089>
- Steinbock, R. T. (1989a). Studies in ancient calcified soft tissues and organic concretions. I: A review of structures, diseases, and conditions. *Journal of Paleopathology*, 3, 35–38.
- Steinbock, R. T. (1989b). Studies in ancient calcified soft tissues and organic concretions. II: Urolithiasis (renal and urinary bladder stone disease). *Journal of Paleopathology*, 3, 39–59.
- Steinbock, R. T. (1990). Studies in ancient calcified soft tissues and organic concretions. III: Gallstones (cholelithiasis). *Journal of Paleopathology*, 3, 95–106.
- Stelmach, R., Pawlowski, M., Klimek, L., & Janas, A. (2016). Biochemical structure, symptoms, location and treatment of sialoliths. *Journal of Dental Sciences*, 11(3), 299–303. <https://doi.org/10.1016/j.jds.2016.02.007>
- Stinton, L. M., & Shaffer, E. A. (2012). Epidemiology of gallbladder disease: Cholelithiasis and cancer. *Gut and Liver*, 6(2), 172–187. <https://doi.org/10.5009/gnl.2012.6.2.172>
- Sun, H., Warren, J., Yip, J., Ji, Y., Hao, S., Han, W., & Ding, Y. (2022). Factors influencing gallstone formation: A review of the literature. *Biomolecules*, 12(4), 550. <https://doi.org/10.3390/biom12040550>
- Tebben, P. J., Singh, R. J., & Kumar, R. (2016). Vitamin D-mediated hypercalcemia: Mechanisms, diagnosis, and treatment. *Endocrine Reviews*, 37(5), 521–547. <https://doi.org/10.1210/er.2016-1070>
- Teymoortash, A., Buck, P., Jepsen, H., & Werner, J. A. (2003). Sialolith crystals localized intraglandularly and in the Wharton's duct of the human submandibular gland: An X-ray diffraction analysis. *Archives of Oral Biology*, 48(3), 233–236. [https://doi.org/10.1016/S0003-9969\(02\)00211-X](https://doi.org/10.1016/S0003-9969(02)00211-X)
- Trotman, B. W. (1991). Pigment gallstone disease. *Gastroenterology Clinics of North America*, 20(1), 111–126. [https://doi.org/10.1016/S0889-8553\(21\)00536-7](https://doi.org/10.1016/S0889-8553(21)00536-7)
- Tsai, C.-C., Chou, H.-H., Wu, T.-L., Yang, Y.-H., Ho, K.-Y., Wu, Y.-M., & Ho, Y.-P. (2008). The levels of volatile sulfur compounds in mouth air from patients with chronic periodontitis. *Journal of Periodontal Research*, 43(2), 186–193. <https://doi.org/10.1111/j.1600-0765.2007.01011.x>
- Turati, M., Anghileri, F. M., Bigoni, M., Rigamonti, L., Tercier, S., Nicolaou, N., & Accadbled, F. (2023). Osteochondritis dissecans of the knee: Epidemiology, etiology, and natural history. *Journal of Children's Orthopaedics*, 17(1), 40–46. <https://doi.org/10.1177/18632521221149063>
- Turner, J. J. O. (2017). Hypercalcaemia—presentation and management. *Clinical Medicine (London, England)*, 17(3), 270–273. <https://doi.org/10.7861/clinmedicine.17-3-270>
- Uozumi, H., Sugita, T., Aizawa, T., Takahashi, A., Ohnuma, M., & Itoi, E. (2009). Histologic findings and possible causes of osteochondritis dissecans of the knee. *American Journal of Sports Medicine*, 37(10), 2003–2008. <https://doi.org/10.1177/0363546509346542>
- Van Offel, J. F., De Clerck, L. S., Franckx, L. M., & Stevens, W. J. (1995). The clinical manifestations of ochronosis: A review. *Acta Clinica Belgica*, 50(6), 358–362. <https://doi.org/10.1080/17843286.1995.11718475>
- Velasco Vázquez, J., Alberto Barroso, V., Delgado-Darias, T., Moreno-Benitez, M. A., Lecuyer, C., & Richardin, P. (2019). Poblamiento, colonización y primera historia de Canarias: El C14 como paradigma. *Anuario de Estudios Atlánticos*, 66, 1–24.
- Velasco-Vazquez, J., Gonzalez-Reimers, E., Arnay-De-La-Rosa, M., Barros-Lopez, N., Martin-Rodriguez, E., & Santolaria-Fernandez, F. (1999). Bone histology of prehistoric inhabitants of the Canary Islands: Comparison between El Hierro and Gran Canaria. *American Journal of Physical Anthropology*, 110(2), 201–213. [https://doi.org/10.1002/\(SICI\)1096-8644\(199910\)110:2<201::AID-AJPA6>3.0.CO;2-N](https://doi.org/10.1002/(SICI)1096-8644(199910)110:2<201::AID-AJPA6>3.0.CO;2-N)
- Ventura, L., Arrizza, L., Quaresima, R., & Capulli, M. (2022). Multidisciplinary investigation of an ancient renal stone in a mummy from Popoli, central Italy. *Pathologica*, 114(4), 339–341. <https://doi.org/10.32074/1591-951X-260>
- Verneau, R. (1879). Habitats et sépultures des anciens habitants des Îles Canaries. *Review d'Anthropologie, 2ème série(T.II)*, 250–264.
- Verrecchia, E. P., Freydet, P., Verrecchia, K. E., & Dumont, J.-L. (1995). Spherulites in calcrete laminar crusts; biogenic CaCO₃ precipitation as a major contributor to crust formation. *Journal of Sedimentary Research*, 65(4a), 690–700. <https://doi.org/10.1306/D426819E-2B26-11D7-8648000102C1865D>
- Williams, J. C. J., Sacks, A. J., Englert, K., Deal, R., Farmer, T. L., Jackson, M. E., Lingeman, J. E., & McAteer, J. A. (2012). Stability of the infection marker struvite in urinary stone samples. *Journal of Endourology*, 26(6), 726–731. <https://doi.org/10.1089/end.2011.0274>
- Yammine, K. (2014). The prevalence of the sesamoid bones of the hand: A systematic review and meta-analysis. *Clinical Anatomy*, 27(8), 1291–1303. <https://doi.org/10.1002/ca.22378>

- Yatera, K., Hanaka, M., Hanaka, T., Yamasaki, K., Nishida, C., Kawanami, T., Kawanami, Y., Ishimoto, H., Kanazawa, T., & Mukae, H. (2015). A rare case of paragonimiasis miyazakii with lung involvement diagnosed 7 years after infection: A case report and literature review. *Parasitology International*, 64(5), 274–280. <https://doi.org/10.1016/j.parint.2015.02.009>
- Zhu, Y., Gao, Y.-H., Zou, J.-N., & Xi, E.-P. (2021). Beware of pleural thickening and calcification: An enlightenment from a case of tuberculous pleurisy. *Risk Management and Healthcare Policy*, 14, 1551–1554. <https://doi.org/10.2147/RMHP.S303614>
- Zúñiga Thayer, R., Suby, J., Flensburg, G., & Luna, L. (2018). Osteocondritis disecante. Primeros Resultados en Restos Humanos de Cazadores-Recolectores del Holoceno en Patagonia Austral. *Revista del Museo de Antropología*, 11, 107–120. <https://doi.org/10.31048/1852.4826.v11.n1.18882>

How to cite this article: Ordóñez, A. C., Suárez-Toste, E., Cockerill, S., González-Reimers, E., & Arnay-de-la-Rosa, M. (2023). SEM technology for the analysis of tiny calcified remains from a pre-Hispanic burial from El Hierro (Canary Islands). *Archaeometry*, 1–17. <https://doi.org/10.1111/arcm.12934>